A NUMERICAL APPROACH FOR 2-D SUTTERBY FLUID-FLOW BOUNDED AT A STAGNATION POINT WITH AN INCLINED MAGNETIC FIELD AND THERMAL RADIATION IMPACTS

by

Zulqurnain SABIR[a], Ali IMRAN[b*], Muhammad UMAR[a], Muhammad ZEB[b], Muhammad SHOAIB[b], Muhammad Asif Zahoor RAJA[c].

[a] Department of Mathematics, Hazara University, Mansehra, Pakistan
[b] Department of Mathematics, COMSATS University Islamabad, Attock, Pakistan
[c] Department of Electrical and Computer Engineering,
COMSATS University Islamabad, Attock, Pakistan

Original scientific paper
https://doi.org/10.2298/TSCI191207186S

The present study investigates the impacts of thermal radiation and inclined magnetic field on the Sutterby fluid by capitalizing Cattaneo-Christov heat flux system. The suitable transformations from PDE into ODE are achieved by capitalizing the strength of similarity conversion system. Well known numerical shooting technique is used along with integrated strength Runge-Kutta method of fourth order. The proposed results are compared with Lobatto 111A method which strengthen the convergence and accuracy of present fluidic system. The skin friction coefficients and Nusselt number are numerically exhibited in tabular form, while the parameter of interests in terms of velocity ratio parameter, power law index, the thermal radiation parameter, Prandtl number, Deborah number, and magnetic parameter. Here in this contemporary investigation, the phenomenon of thermal radiation on an inclined magnetic field using Sutterby capitalizing Cattaneo-Christov heat flux model has been discussed. The resulting complex non-linear ODE are tackled numerically by utilizing a famous shooting technique with the integrated strength of the Runge-Kutta method of fourth order. The obtained numerical results are compared with the MATLAB built-in solver bvp4c. The numerical values of the skin friction coefficient and reduced Nusselt number are narrated in tabular form, while some proficient parameters like velocity ratio parameter, power-law index, Deborah number, magnetic parameter, inclined magnetic angle, the thermal radiation parameter, Reynolds number, and Prandtl number on the velocity and temperature profiles have been discussed numerically as well as graphically. Outcomes of the proposed research show that by increasing the inclined angle, enhancement is seen in the skin-friction coefficient and reduces the Nusselt number. Moreover, by increasing the Reynolds number, the temperature profile declines initially and then moves upward in the channel. The stability and convergence of the proposed methodolgy in validated through residual errors based different tolerances.

Key words: *sutterby fluid, inclined magnetic field, , skin-friction coefficient, reduced Nusselt number, heat flux model, thermal radiation*

Introduction

The appliance of heat transfer governs a crucial part in magnetic drug targeting, cooling nuclear reactors, thermal managing of electronic procedures, conduction of heat in tissues, *etc*.

* Corresponding author, e-mail: ali.imran@cuiatk.edu.pk

Aforementioned researchers studied mechanism with the help of Fourier law [1]. This law has the disadvantage of quantifying the preliminary disturbance promptly within entire medium and due to this main argument, the Fourier law forms a parabolic scenario for the profile of temperature. Cattaneo [2] promoted the heat conduction law by integrating a thermal relaxation factor and produced the transformation of heat in the thermal wave form. Christov [3] comprised Oldroyd's upper convected derivative in place of time derivative and his work is based on Cattaneo-Christov heat flux model. Furthermore, Han *et al*. [4] observed the transfer of heat in the Maxwell fluid slip flow in light using the Cattaneo-Christov model. Mustafa [5] carries out the upper convected Maxwell fluid-flow study. Some recent efforts were also presented in [6-8].

Many fluids having non-Newtonian nature is encountered in industrial, biological and engineering procedures. Due to the diverse utilities of such non-Newtonian nature fluids, various studies have been carried out using the rheological possessions of these fluids. Governing momentum equations for Newtonian fluid are not enough to define the nature of these complex fluids like oil reservoir, cosmetic, nuclear industries, clay coating, polymer melts, suspended liquids, paints, gasoline, *etc*. The models that are used normally in the non-Newtonian fluid are, the Maxwell fluid model, the second grade model, power law model and Oldroyd-B model. Fetecau *et al*. [9] investigated unsteady flow of a Maxwell fluid using fractional derivative model, in annular cylinder. Yin *et al*. [10] focused on thermal convective viscoelastic Couette flow in a horizontal plane. Makinde *et al*. [11] examined the thermal effects for unsteady flow of a pressure driven, variable viscosity, third-grade fluid through a permeable asymmetrical channel. Rashidi and Abbasbandy [12] presented analytical solution for heat transfer of a micropolar fluid near a permeable medium with radiation. The power-law fluid type of models have been diversely used in examining the rheological phenomena of such kind of fluids. In recent years, the model of the Sutterby fluid-flow [13, 14] has achieved the attention of researchers due to the comprehensive mathematical behavior and its significance to validate the phenomena of dilatant fluids as well as pseudoplastic. The observations of boundary-layer flow are recorded in various industrial settings like liquid films, synthetic sheets extrusion, glass industry, metallic plate manufacturing and condensation, *etc*. First time Sakiadis [15] discussed the occurrence of stretching flow, and after some years very much attention is given to the characteristics of stretching flows. Cortell [16] has developed the similarity solution and examined the effects of heat transfer and hydromagnetic-flow over on extended factor. Moreover, Chakrabarti and Gupta [17] have investigated in the same direction. Keeping the worth of their work, Andersson *et al*. [18] extended to power-law fluid. It is important to mention here that the production of papers, continuous casting and glass blowing, heat transfer and stagnation point flow are determined. Chiam [19] discussed the viscous flow of stagnation point to the surface of linear enlarging. Ishak *et al.* [20] examined the combined convection flow of stagnant point near a porous stretching sheet. Mahpatra and Gupta [21] studied the analysis of thermodynamics using a stagnation point flow in the vicinity of stretching surface. In recent time, Oahimirea and Olajuwonb [22] discussed the heat conduction for hydromagnetic flow based on stagnation point and stretching surface. Weidman [23] presented the axisymmetric gyratory flow based on radially stretching sheet and stagnation point. Vajravelu *et al*. [24] worked on the Hall current influence on transfer of heat and MHD flow past a narrow stretching sheet along with variant fluid characteristics. Pal *et al*. [25] emphasized on experimental analysis of nanofluids on a non-linear stretching/shrinking sheet. Iqbal *et al*. [26] investigated the impact of MHD on nanofluidic fluid-flow problem at a stagnation point. Iqbal *et al*. [27] numerical investigated the stagnation point flow of CNT using induced magnetic field engulfed in bioconvection nanoparticles. Iqbal *et al*. [28] in another study inspected the impact of MHD and entropy generated

flow of nanofluid. Meraj *et al*. [29] presented in their study debate on the ferrofluidic flow over a dynamic surface manipulated by a magnetic dipole. Iqbal *et al*. [30] investigated the effect of heat convective nanofluid-flow over a moving Riga plate of variant thickness. Stagnation point flow for a non-Newtonian fluid by utilizing the Cattaneo-Christov heat flux model is presented by Azhar *et al*. [31]. Iqbal *et al*. [32] analyzed the MHD rotating flow of CNT in a transverse channel, engulfed with Hall current and oscillations. A shooting technique for investigation of the 3-D Eyring-Powell fluid with activation energy over a stretching sheet with slip has been examined by Umar *et al*. [33].

When the coefficient of heat transfer is trivial, thermal radiation effect plays more vibrant role in the whole surface. The phenomenon of thermal radiation for diverse convection through a vertical surface by utilizing a permeable medium was discussed by Bakier [34]. The author used Runge-Kutta method of fourth order to tackle the leading equations. Damseh [35] examined numerically the effects of MHD on the mixed convection fluid-flow along a radiative surface based on porous medium. By applying the implicit iterative finite difference scheme, the author tackled the unit-less boundary-layer model. Here it is worth mentioning to describe that the results of thermal radiation are significant in high temperature and space technology procedures. Thermal radiation mechanism possess a vibrant role in the procedural management of heat in the industry of polymer processing. Hossain and Takhar [36] investigated the radiation effects by utilizing heat transfer models. Zahmatkesh [37] has established that the occurrence of thermal radiation transforms the temperature division approximately alike in the transverse units in the field and makes the streamlines to be almost parallel. Moradi *et al*. [38] showed the thermal study of combined convection radiation of a flat inclinedly held plate rooted in a permeable cross-section. Moreover, the impact of radiation on the convective flow along a transverse wall in a porous medium is examined by Pal and Mondal [39]. In general, in the modern sophisticated technology submissions such as nuclear reactor refrigeration, the structure reactor is designed as a heat manufacture permeable, satisfying the convective flow. Bahmani and Kargarsharifabad [40, 41] investigated the MHD free convective flow of power-law fluids near a horizontal plate due to a constant heat flux. Waqar *et al*. [42] studied buoyancy flows of third grade nanofluids near a vertical porous stretching sheet and investigated the numerical solution. Ibrahim and Makinde [43] explored the impacts of velocity slip and convective heating, along with Brownian motion and thermophoresis effects on the MHD stagnation point flow by utilizing the power-law nanofluid. Oblique hydromagnetic-flow near stagnation point for temperature variant viscosity using MHD Newtonian nanofluid with of thermal radiation effects has been studied by Khan *et al*. [44]. Ibrahim and Makinde [45] and Makinde *et al*. [46] in their study presented the effect of slip and convective boundary condition on MHD stagnation point flow with heat transfer for Casson nanofluid. Makinde *et al*. [47] analyzed the flow of nanofluid with phenomenon of buoyancy force, Brownian motion, convective heating, thermophoresis, and MHD near stagnation point with heat effects.

Sutterby fluid [13] is one of the very important non-Newtonian fluids which represents constitutive equations of high polymer acqueous solutions. The results of current investigation will be significant for the applications in polymer manufacturing industries. In this study, a numerical solution of the Sutterby fluid by exploiting Cattaneo-Christov heat flux model with inclined magnetic field and thermal radiation effects is presented. The motivation behind the fact that the non-Newtonina Sutterby fluid model is chosen to observe the rheological properties of shear thinning/thickening with the impacts of thermal radiation and inclined MHD. To investigate the behavior of velocity ratio parameter, power-law index, Deborah number, magnetic parameter, inclined magnetic angle, the thermal radiation parameter, Prandtl number,

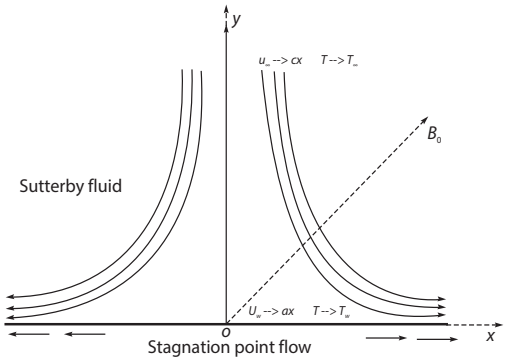

Figure 1. Flow diagram

and Reynolds number, well known shooting scheme along with 4th order Runge-Kutta technique is discussed.

Problem formulation

Consider the 2-D flow of Sutterby fluid over a stretching sheet with an inclined MHD and thermal radiation characteristics. The stretching surface is considered in line with the *x*-axis while *y*-axis is taken perpendicular to it. The transport of physical phenomenon for both boundary-layer and stretching flows is provided in fig. 1. The governing equations for the Sutterby fluid [13] flow are given [48]:

$$u\frac{\partial u}{\partial x}+v\frac{\partial u}{\partial y}=U_e\frac{\partial U_e}{\partial x}+\frac{\mu_0}{\rho}\left[\frac{\partial^2 u}{\partial y^2}+mB^2\left(\frac{\partial u}{\partial y}\right)^2\frac{\partial^2 u}{\partial y^2}\right]-\frac{\sigma}{\rho}B_0^2\left(u-U_e\right)\sin^2\vartheta \tag{1}$$

with the relevant boundary conditions

$$\begin{aligned} u=U_w\left(x\right)=ax,\quad v=0,\quad \text{at } y=0\\ u=U_e\left(x\right)=cx,\quad u'\left(y\right)\to 0 \text{ as } y\to\infty \end{aligned} \tag{2}$$

where m shows three conditions. If $m < 0$, then it shows pseudoplastic or represents fluid with deceasing viscosity, $m > 0$, demonstrates the dilatant or fluid with increasing viscosity and $m = 0$ reflects Newtonian fluid. Numerous fluids can be discussed by taking various power-law index values. we have taken the transport of heat in the fluid, conduction dominated. Therefore, we have neglected convection and viscous dissipation. Moreover, in the case of stretching sheet flow is weak and therefore, viscous dissipation and Joule heating has negligible effect. The expression of Cattaneo-Christov heat flux model [3-6]:

$$\lambda_3\left[\frac{\partial q}{\partial t}-\left(\nabla V\right)q+V\nabla q-q\nabla V\right]+q=-k\nabla T \tag{3}$$

Using the aforementioned eq. (4), the energy equation [48] takes the form:

$$\begin{aligned} &\left(u\frac{\partial}{\partial x}+v\frac{\partial}{\partial y}\right)T+\lambda_3\left(u\frac{\partial u}{\partial x}\frac{\partial}{\partial x}+u\frac{\partial v}{\partial y}\frac{\partial}{\partial y}+v\frac{\partial v}{\partial y}\frac{\partial}{\partial y}+v\frac{\partial u}{\partial y}\frac{\partial}{\partial x}+\right.\\ &\left.+u^2\frac{\partial^2}{\partial x^2}+v^2\frac{\partial^2}{\partial y^2}+2uv\frac{\partial^2}{\partial x\partial y}\right)T=\alpha\frac{\partial^2 T}{\partial y^2}\left(1+\frac{16\sigma^* T_\infty^3}{3kk^*}\right) \end{aligned} \tag{4}$$

and the boundary conditions:

$$T=T_w,\text{ on } y=0,\ T=T_\infty,\text{ when } y\to\infty \tag{5}$$

The transformation for the proposed system:

$$u=axf'\left(\eta\right),\ v=-\sqrt{av}f\left(\eta\right),\ \eta=\sqrt{\frac{a}{\nu}}y^2,\ \theta\left(\eta\right)=\frac{T-T_w}{T_\infty-T_w}$$

By capitalizing the previous similarity transforms, the aforementioned PDE (1), (2), and (6) take the form:

$$f''' + ff'' - f'^2 + 0.5m\mathrm{De}\mathrm{Re}f''^2 f''' - M\left(f' - A\right)\sin^2\vartheta + A^2 = 0 \tag{6}$$

$$\left(1 + \frac{4}{3}Nr\right)\theta'' + \mathrm{Pr}\left(f\theta' - \gamma ff'\theta' - \gamma f^2\theta''\right) = 0 \tag{7}$$

The concerning boundary conditions:

$$\begin{gathered} f(0) = 0, \quad f'(0) = 1, \quad \theta(0) = 1 \quad \text{at } \eta = 0 \\ f'(\eta) = A, \quad \theta(\eta) = 0 \quad \text{as } \eta \to \infty \end{gathered} \tag{8}$$

The expressions for the aforementioned dimensionless numbers:

$$\mathrm{Re} = \frac{ax^2}{\nu},\ A = \frac{c}{a},\ \mathrm{De} = B^2a^2,\ \gamma = \lambda_3 a,\ M = \frac{\sigma B_0^2}{a\rho},\ \mathrm{Pr} = \frac{\nu}{\alpha},\ Nr = \frac{4\sigma^* T_\infty^3}{K^* K_f} \tag{9}$$

The skin friction coefficient, C_{fx}, and Nusselt number, Nu_x, are interpreted:

$$\mathrm{Re}_x^{0.5} C_{fx} = f''(0),\ \frac{\mathrm{Nu}_x}{\mathrm{Re}_x^{0.5}} = -\theta'(0) \tag{10}$$

Methodology

An overview is presented for the solution of non-linear ODE (8) and (9) w.r.t. the boundary conditions (10) in this section. The solution of these non-linear ODE has been presented by using a famous technique named as shooting technique. The numerical outcomes are analyzed with the bvp4c that is built-in solver in MATLAB and the domain is taken as $[0, \eta_{\max}]$. The representations f by y_1 and θ by y_4 have been implemented to convert the BVP into IVP:

$$\begin{aligned} y_1' &= y_2, & y_1(0) &= 0 \\ y_2' &= y_3, & y_2(0) &= 1 \\ y_3' &= \frac{y_2^2 - y_1y_3 + M\left(y_2 - A\right)\sin^2\vartheta - A^2}{1 + 0.5m\mathrm{Re}y_3^2}, & y_3(0) &= i_1 \\ y_4' &= y_5, & y_4(0) &= 1 \\ y_5' &= \frac{\mathrm{Pr}\left(\gamma y_1y_2y_5 - y_1y_5\right)}{1 + \frac{4}{3}Nr - \gamma\mathrm{Pr}y_1^2}, & y_5(0) &= i_2 \end{aligned} \tag{11}$$

The solution of the previous IVP is presented by using a famous shooting technique along with Runge-Kutta scheme. The missing initial conditions are denoted as $y_3(0) = i_1$ and $y_5(0) = i_2$. The traditional Newton's scheme is functional for the improvement of missing initial conditions. The shooting's numerical scheme is applied for the missing values of i_1 and i_2 until it cannot meet the tolerance:

$$\max\left\{\left|y_3\left(\eta_{\max}\right)\right|, \left|y_5\left(\eta_{\max}\right)\right|\right\} < \xi \tag{12}$$

where $\xi > 0$ is very small number and its value is selected as $\xi = 10^{-7}$.

A critical analysis of the present results of $f''(0)$ and $-\theta'(0)$ for the velocity ratio parameter A and Deborah number w.r.t heat flux Deborah number using the bvp4c is provided in tab. 1. The critical analysis of these numerical results in tab. 1 shows the correctness of the scheme, $m = 1.5$, Re = De = 1, Pr = $Nr = 0.1$, and $\vartheta = 0$.

Table 1. Comparison of the numerical results

	bvp4c	Present		bvp4c	Present
A	$f''(0)$	$f''(0)$	γ	$-\theta'(0)$	$-\theta'(0)$
	–0.88588	–0.88588	0	0.24374	0.24374
0.1	–0.88611	–0.88611	0.2	0.24358	0.24358
0.2	–0.88678	–0.88678	0.4	0.24311	0.24311
0.3	–0.88786	–0.88786	0.6	0.24242	0.24242
0.4	–0.88930	–0.88930	0.8	0.24164	0.24164
0.5	–0.89106	–0.89106	1	0.24087	0.24087
0.6	–0.89305	–0.89305	1.2	0.24025	0.24025
0.7	–0.89520	–0.89520	1.4	0.23986	0.23986
0.8	–0.89741	–0.89741	1.6	0.23975	0.23975
0.9	–0.89960	–0.89960	1.8	0.23994	0.23994
1.0	–0.90169	–0.90169	2	0.24041	0.24041

The comparison of results in tab. 1 indicates the impressively substantial arrangements of the current investigation with the bvp4c results, that motivate the author to solve this problem with the variations of thermal radiation and inclined MHD effects by using a famous shooting technique.

Results and discussions

The physical measures of the coefficient of skin-friction and the reduced Nusselt number are tabulated in tab. 2. Here it important to mention that the coefficient of the skin friction reduces for velocity ratio parameter, A, and power law flow behavior indicator, m, while the opposite variation of both of the parameters is seen for the reduced Nusselt number. The coefficient of skin-friction increases for the inclined magnetic field, ϑ, and opposite effects are noticed for reduced Nusselt number. Moreover, the skin friction values for Reynolds number, and Deborah number, give the same decreasing impact, whereas small increasing behavior for both of the parameters is seen in reduced Nusselt number. The values of the coefficient of skin-friction for Prandtl number, increases, while opposite effects are for the Deborah number for heat flux, γ, and radiation parameter, Nr. The tab. 3 shows the convergence and accuracy of the proposed scheme through the residual errors with variants of tolerances which prove the worth of the scheme.

In order to have more in depth understanding, the impacts of different parameter on non-dimension velocity and temperature profiles which mathematically written as $f'(\eta)$ and $\theta(\eta)$ are exhibited in this section. The variations of important physical parameters on $f'(\eta)$ and $\theta(\eta)$ are demonstrated in figs. 2-11. The velocity representations for various values of velocity ratio parameter, A, are provided in fig. 2. By increasing the values of A, increment is noticed in the velocity profile, which is due to the reason that stretchable velocity at the surface is higher, in comparison the stagnation velocity of the exterior stream. Then development in the thickness

Table 2. Values of $\mathrm{Re}_x^{0.5} C_f = -f''(0)$ and $\mathrm{Re}_x^{0.5} \mathrm{Nu}_x = -\theta'(0)$ for different parameters

									$-\mathrm{Re}_x^{0.5} C_f$		$-\mathrm{Re}_x^{0.5} \mathrm{Nu}_x$	
A	m	ϑ	Re	De	M	Pr	γ	Nr	Shooting	bvp4c	Shooting	bvp4c
0.1	0.1	0	1	0.1	0.1	0.1	0.1	0.1	0.96831	0.96831	0.16726	0.16726
0.2									0.91719	0.91719	0.17419	0.17419
0.3									0.84869	0.84869	0.18181	0.18181
0.4									0.76479	0.76479	0.18990	0.18990
	0.5								0.66550	0.66550	0.19835	0.19835
	1								0.66375	0.66375	0.19836	0.19836
	1.5								0.66205	0.66204	0.19837	0.19837
		π/6							0.97666	0.97666	0.16710	0.16710
		π/4							0.98494	0.98494	0.16695	0.16695
		π/3							0.99316	0.99316	0.16680	0.16680
			3						0.96618	0.96618	0.16728	0.16728
			6						0.96305	0.96305	0.16731	0.16731
			9						0.95999	0.95999	0.16733	0.16733
				0.5					0.96409	0.96409	0.16730	0.16730
				0.9					0.95999	0.95999	0.16733	0.16733
				1.3					0.95602	0.95602	0.16737	0.16737
					1.0				0.96831	0.96831	0.16726	0.16726
					2.0				0.96831	0.96831	0.16726	0.16726
					3.0				0.96831	0.96831	0.16726	0.16726
						0.3			0.96831	0.96831	0.26224	0.26224
						0.5			0.96831	0.96831	0.35784	0.35784
						0.7			0.96831	0.96831	0.44623	0.44623
							0.4		0.96831	0.96831	0.16593	0.16593
							0.7		0.96831	0.96831	0.16461	0.16461
							1		0.96831	0.96831	0.16328	0.16328
								0.3	0.96831	0.96831	0.15881	0.15881
								0.5	0.96831	0.96831	0.15316	0.15316
								0.7	0.96831	0.96831	0.14912	0.14912

of the boundary-layer is noticed with the enhancement in A. Here $A = 1$ represents to the state when stagnation velocity of the exterior stream coincides with the fluid stretching velocity. Moreover, it is quite evident that the boundary-layer flow thickness is declined for those values of $A > 1$. The graph for different values of power-law behavior index m is plotted in fig. 3. The case when $m < 0$ shows a pseudoplastics behavior, $m = 0$ results the Newtonian type of fluid and $m > 0$ represents a Dilatant fluid behavior. Figures 4-5 show the fluidity representations of Deborah number for the cases when $m > 0$ and $m < 0$. Increments in the values of Deborah number show the opposite behavior of the velocity fields for both cases.

By increasing the values of Deborah number, the flow of fluid accelerates, on other hand reduces for higher values of Deborah number in the form for the pseudoplastic fluid.

Table 3. Relative error encountered during computations of $f'(\eta)$

Scenarios	Case 1	Case 2	Case 3	Case 4
1	De = 1	De = 4	De = 7	De = 10
2	$A = 0.1$	$A = 0.2$	$A = 0.3$	$A = 0.4$
3	$m = 0$	$m = 3$	$m = 6$	$m = 9$
4	$M = 1$	$M = 2$	$M = 3$	$M = 4$
5	$\theta = 30$	$\theta = 45$	$\theta = 60$	$\theta = 90$
6	De = 0.1	De = 0.2	De = 0.3	e = 0.4

Tolerance	Scenarios	Case 1	Case 2	Case 3	Case 4
10^{-6}	1	$5.4040969431 \cdot 10^{-10}$	$1.0843427772 \cdot 10^{-9}$	$2.9393362752 \cdot 10^{-9}$	$4.2081307183 \cdot 10^{-9}$
	2	$9.2203768595 \cdot 10^{-8}$	$1.9481657028 \cdot 10^{-8}$	$1.7338434791 \cdot 10^{-8}$	$1.4819070657 \cdot 10^{-8}$
	3	$1.1459266748 \cdot 10^{-7}$	$2.0955693606 \cdot 10^{-8}$	$1.6135248539 \cdot 10^{-8}$	$7.9155988877 \cdot 10^{-9}$
	4	$1.3913045977 \cdot 10^{-7}$	$1.8367605405 \cdot 10^{-7}$	$2.3159913164 \cdot 10^{-7}$	$2.6405362344 \cdot 10^{-7}$
	5	$1.3913045977 \cdot 10^{-7}$	$1.8367605407 \cdot 10^{-7}$	$2.3159913170 \cdot 10^{-7}$	$2.6405472819 \cdot 10^{-7}$
	6	$1.0038593961 \cdot 10^{-7}$	$9.9763532626 \cdot 10^{-8}$	$9.9147113187 \cdot 10^{-8}$	$9.8536644297 \cdot 10^{-8}$
10^{-12}	1	$5.4036556158 \cdot 10^{-16}$	$1.0843427590 \cdot 10^{-8}$	$2.9393366629 \cdot 10^{-15}$	$4.2081305374 \cdot 10^{-15}$
	2	$9.2220621941 \cdot 10^{-14}$	1.9481657028e-14	$1.7338432243 \cdot 10^{-14}$	$1.4819069140 \cdot 10^{-14}$
	3	$1.1761911777 \cdot 10^{-13}$	$2.0955693586 \cdot 10^{-14}$	$1.6134516711 \cdot 10^{-14}$	$7.9155792715 \cdot 10^{-15}$
	4	$1.5306858777 \cdot 10^{-13}$	$2.2543186668 \cdot 10^{-13}$	$3.1393773309 \cdot 10^{-13}$	$2.6405362344 \cdot 10^{-13}$
	5	$1.5306858777 \cdot 10^{-13}$	$2.2543186668 \cdot 10^{-13}$	$3.1393773311 \cdot 10^{-13}$	$2.6405472819 \cdot 10^{-13}$
	6	$1.0051876986 \cdot 10^{-13}$	$9.9886063235 \cdot 10^{-14}$	9.9259675333e·10^{-14}	$9.8639563926 \cdot 10^{-14}$

Surge in the values of Deborah number has a vital role in refining elastic impacts, as a result dilatant fluids makes to improve fluid-flow, quite different behavior is observed for the pseudoplastic fluid. Velocity profile is deceasing function of M, which is given in fig. 6. The cause is behind the statement is the drag forces named as Lorentz forces, which makes to oppose the fluid due to this decrements is noticed in the velocity profile. Some useful findings of inclined magnetic field using the inclined angle, ϑ, on velocity field are plotted in fig. 7. It is quiet clear from the figure that velocity profile reduces with increasing the values of inclination angle, ϑ. With the augmentation in inclination angle, an enhancement is seen in the magnetic field effects on fluid particles which consequently strengthens the Lorentz force that cause the decrements in the velocity profile. Figure 8 exhibits declining trend in thermal boundary-layer thickness and temperature for higher value of γ. The fluid which has larger relaxation time shows lesser temperature and the fluid has lesser heat flux relaxation time leads to larger temperature. The variations of Prandtl number on temperature distribution is examined in fig. 9. It is noticed that the significant rise in the value of Prandtl number weakens the temperature profile as a result decrements is seen in the thermal boundary-layer, due to this reason if Prandtl number is increased the thermal conductivity depreciates. One can observed that in the beginning the temperature profile decreases and then it increases throughout the whole interval. The increasing and decreasing comportment of the temperature distribution for various values

of the radiation parameter, *Nr*, is narrated in fig. 10. The effects of Reynolds number on the temperature profile are narrated in fig. 11. One may conclude that the thickness of thermal boundary-layer depreciates with the enhancement in Reynolds number. For fluids with decreasing viscosity, a rise in Reynolds number demonstrates an important role in enhancing the viscous as well as elastic phenomenon which takes to an improvement in viscous boundary-layer.

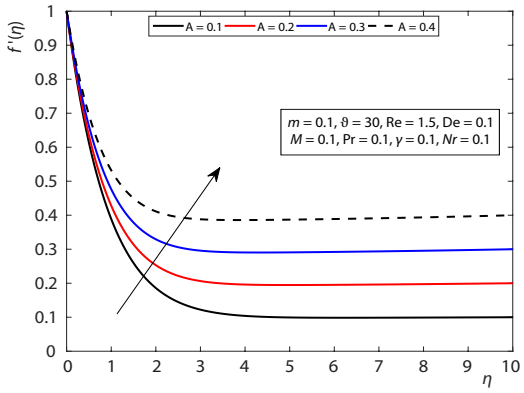

Figure 2. Variation of *A* on *f′*

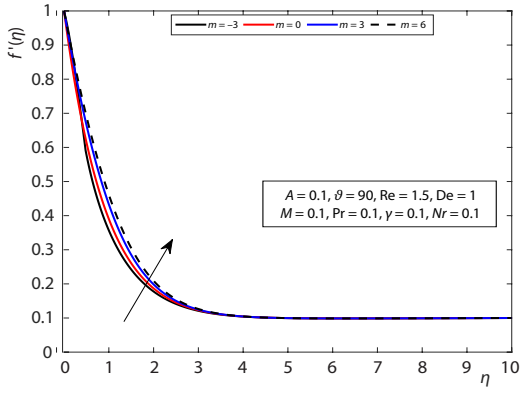

Figure 3. Variation of *m* on *f′*

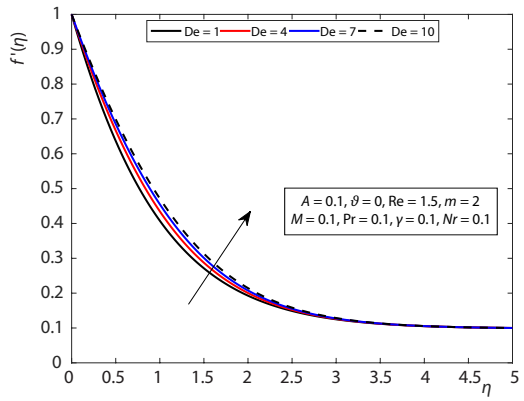

Figure 4. Variations of De on *f′* for *m* > 0

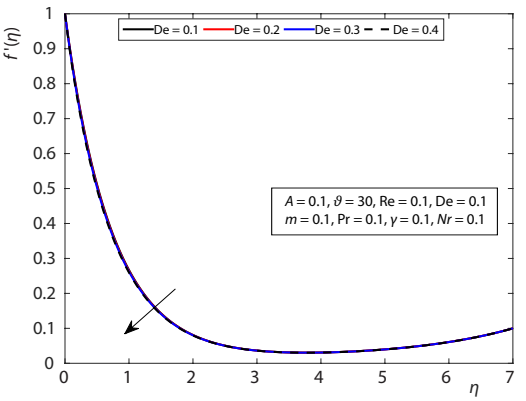

Figure 5. Impacts of De on *f′* for *m* < 0

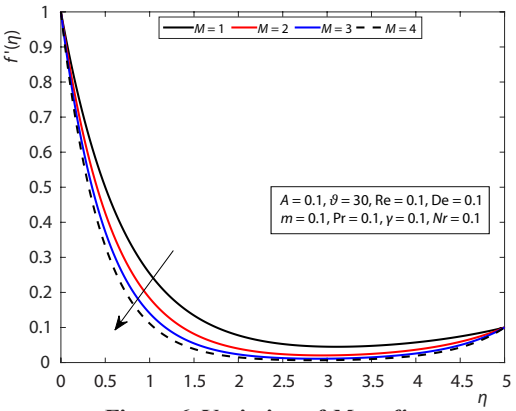

Figure 6. Variation of *M* on *f′*

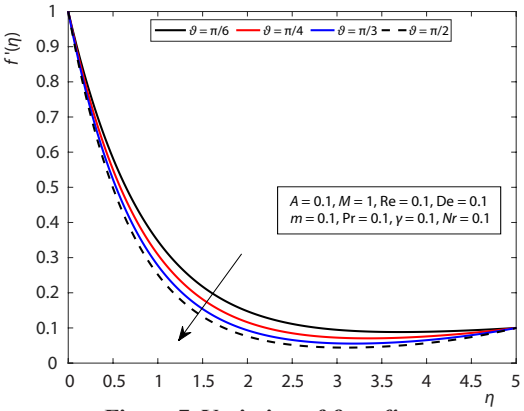

Figure 7. Variation of *ϑ* on *f′*

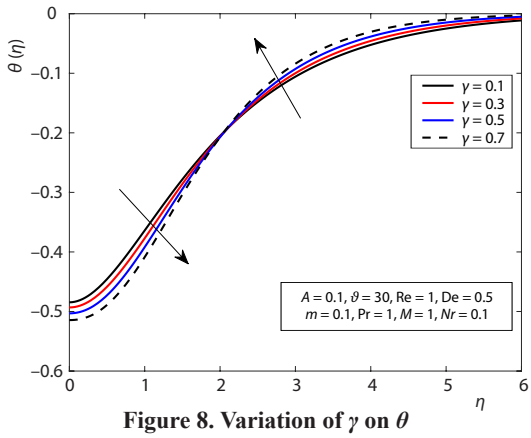

Figure 8. Variation of γ on θ

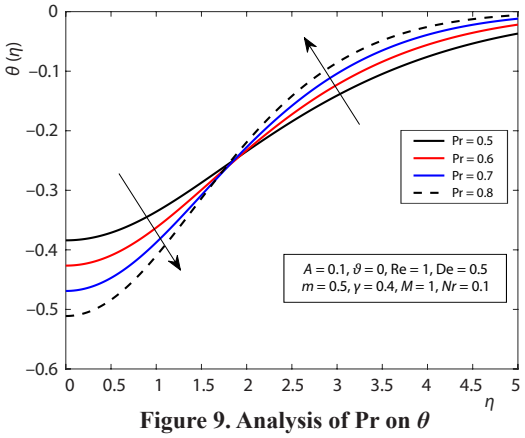

Figure 9. Analysis of Pr on θ

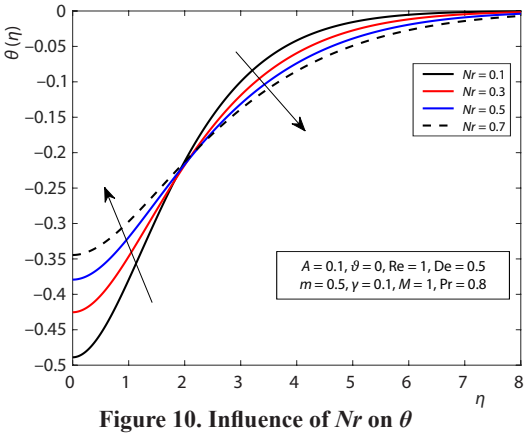

Figure 10. Influence of *Nr* on θ

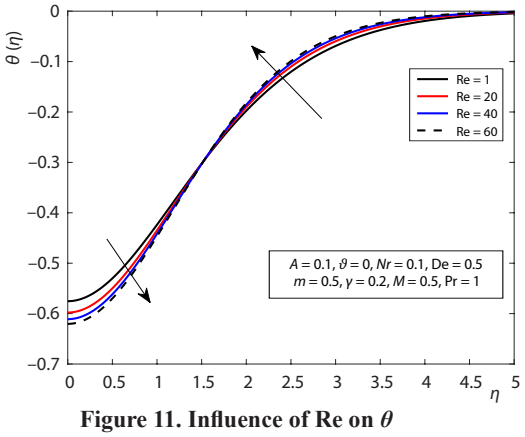

Figure 11. Influence of Re on θ

Conclusions

An effort is made in the contemporary investigation numerically explore different aspects of 2-D Sutterby fluid-flow over a stretching sheet bounded by stagnation point with inclined magnetic field and thermal radiation phenomenon. The strength of similarity conversions is utilized to transform PDE of the fluidic systme into ODE. Which are further handled by capitalizing a famous technique named as shooting technique along with 4th order Runge-Kutta methodology. The achieved numerical consequences are matched with the bvp4c outcomes that proved very good agreements. The software MATLAB R2017(a) package is applied for solving coupled non-linear differential equations. The following conclusions are drawn.

- The Sutterby fluid-flow over a stretching sheet bounded by stagnation point along with the effects of inclined magnetic field and thermal radiations is successfully solved using a renowned shooting methodology.
- The present numerical outcomes are compared with the bvp4c that are found in very good agreements.
- Nusselt number depreciates with an enhancement in the Prandtl number.
- By increasing the inclined angle, enhancement is seen in the skin-friction coefficient and reduces the Nusselt number.
- Nusselt number decreases by increasing the radiation parameter.
- Velocity profile decreased by reinforcing the Hartmann number.

- By taking the large number of Reynolds number, temperature profile declines initially and then as move upward in the channel it enhances.

Nomenclature

A – velocity ratio parameter
a, c – positive constants
B – material constant
B_0 – constant magnetic field
De – Deborah number
K – thermal conductivity
m – power law index
Nr – radiation parameter
Pr – Prandtl number
q – heat flux
Re – Reynolds number
T – temperature
T_∞ – ambient temperature
T_w – constant temperature
t – time
$U_e(x)$ – free stream velocity
u, v – velocity components
$U_w(x)$ – stretching sheet velocity
V – velocity vector

Greek symbols

α – thermal diffusivity
γ – Deborah number for heat flux
λ_3 – relaxation time
μ_0 – fluid viscosity
ρ – fluid density
σ – electrical conductivity
ϑ – inclined angle

References

[1] Baron Fourier, J. B. J., Théorie analytique de la chaleur (in French), F. Didot, 1822
[2] Cattaneo, C., Sulla conduzione del calore (in Italian), Atti Sem. Mat. Fis., Univ. Modena, Vol. 3, pp. 83-101, 1948
[3] Christov, C. I., On Frame Indifferent Formulation of the Maxwell-Cattaneo Model of Finite-Speed Heat Conduction, *Mechanics Research Communications*, *36* (2009), 4, pp. 481-486
[4] Han, S., *et al*., Coupled Flow and Heat Transfer in Viscoelastic Fluid with Cattaneo-Christov Heat Flux Model, *Applied Mathematics Letters*, *38* (2014), Dec., pp. 87-93
[5] Mustafa, M., Cattaneo-Christov Heat Flux Model for Rotating Flow and Heat Transfer of Upper-Convected Maxwell Fluid, *Aip Advances*, *5* (2015), 4, 047109
[6] Azhar, E., *et al*., Numerical Approach for Stagnation Point Flow of Sutterby Fluid Impinging to Cattaneo-Christov Heat Flux Model, *Pramana*, *91* (2018), 5, 61
[7] Hayat, T., *et al*., Modern Aspects of Homogeneous-Heterogeneous Reactions and Variable Thickness in Nanofluids through Carbon Nanotubes, *Physica E: Low-Dimensional Systems and Nanostruc*tures, *94*, (2017), Oct., pp. 70-77
[8] Sabir, Z., *et al*., A Computational Analysis of Two-Phase Casson Nanofluid Passing a Stretching Sheet Using Chemical Reactions and Gyrotactic Microorganisms, *Mathematical Problems in Engineering*, *2019* (2019), ID 1490571
[9] Fetecau, C., *et al*., Flow of Fractional Maxwell Fluid between Coaxial Cylinders, *Archive of Applied Mechanics*, *81* (2011), 8, pp. 1153-1163
[10] Yin, C., *et al*., Thermal Convection of a Viscoelastic Fluid in a Fluid-Porous System Subjected to a Horizontal Plane Couette Flow, *International Journal of Heat and Fluid-Flow*, *44* (2013), Dec., pp. 711-718
[11] Makinde, O. D., *et al*., Unsteady Flow of a Reactive Variable Viscosity Non-Newtonian Fluid through a Porous Saturated Medium with Asymmetric Convective Boundary Conditions, *Computers and Mathematics with Applications*, *62* (2011), 9, pp. 3343-3352
[12] Rashidi, M. M., Abbasbandy, S., Analytic Approximate Solutions for Heat Transfer of a Micropolar Fluid through a Porous Medium with Radiation, *Communications in Non-Linear Science and Numerical Simulation*, *16* (2011), 4, pp. 1874-1889
[13] Sutterby, J. L., Laminar Converging Flow of Dilute Polymer Solutions in Conical Sections – Part I: Vicosity Data, New Viscosity Model, Tube Flow Solution, *AIChE Journal*, *12* (1966), 1, pp. 63-68
[14] Batra, R. L., Eissa, M., Helical flow of a Sutterby Model Fluid, *Polymer-Plastics Technology and Engineering*, *33* (1994), 4, pp. 489-501
[15] Sakiadis, B. C., Boundary-Layer Behavior on Continuous Solid Surfaces: I. Boundary-Layer Equations for 2-D and Axisymmetric Flow, *AIChE Journal, 7* (1961), 1, pp. 26-28
[16] Cortell, R., Similarity Solutions for Flow and Heat Transfer of a Viscoelastic Fluid over a Stretching Sheet, *International Journal of Non-Linear Mechanics*, *29* (1994), 2, pp. 155-161

[17] Chakrabarti, A., Gupta, A. S., Hydromagnetic-Flow and Heat Transfer over a stretching sheet, *Quarterly of Applied Mathematics*, *37* (1979), 1, pp. 73-78
[18] Andersson, H. I., *et al*., Magnetohydrodynamic Flow of a Power-Law Fluid over a Stretching Sheet, *International Journal of Non-Linear Mechanics*, *27* (1992), 6, pp. 929-936
[19] Chiam, T. C., Stagnation-Point Flow Towards a Stretching Plate, *Journal of the Physical Society of Japan*, *63* (1994), 6, pp. 2443-2444
[20] Ishak, A., *et al*., The Effects of Transpiration on the Flow and Heat Transfer over a Moving Permeable Surface in a Parallel Stream, *Chemical Engineering Journal*, *148* (2009), 1, pp. 63-67
[21] Mahapatra, T. R., Gupta, A. S., Heat Transfer in Stagnation-Point Flow Towards a Stretching Sheet, *Heat and Mass Transfer*, *38* (2002), 6, pp. 517-521
[22] Oahimire, J. I., Olajuwon, B. I., Hydromagnetic-Flow Near a Stagnation Point on a Stretching Sheet with Variable Thermal Conductivity and Heat Source/Sink, *International Journal of Applied Science and Engineering*, *11* (2013), 3, pp. 331-341
[23] Weidman, P., Axisymmetric Rotational Stagnation Point Flow Impinging on a Radially Stretching Sheet, *International Journal of Non-Linear Mechanics*, *82* (2016), June, pp. 1-5
[24] Vajravelu, K., *et al*., Influence of Hall Current on MHD Flow and Heat Transfer over a Slender Stretching Sheet in the Presence of Variable Fluid Properties, *Communications in Numerical Analysis*, *1* (2016), 1, pp. 17-36
[25] Pal, D., *et al*., Mixed Convection Stagnation-Point Flow of Nanofluids over a Stretching/Shrinking Sheet in a Porous Medium with Internal Heat Generation/Absorption, *Commun. Numer. Anal*, *2015* (2015), 1, pp. 30-50
[26] Iqbal, Z., *et al*., A Novel Development of Hybrid (MoS_2-SiO_2/H_2O) Nanofluidic Curvilinear Transport and Consequences for Effectiveness of Shape Factors, *Journal of the Taiwan Institute of Chemical Engineers*, *81* (2017), Dec., pp. 150-158
[27] Iqbal, Z., *et al*., Transport Phenomena of Carbon Nanotubes and Bioconvection Nanoparticles on Stagnation Point Flow in Presence of Induced Magnetic Field, *Physica E: Low-Dimensional Systems and Nanostructures*, *91* (2017), July, pp. 128-135
[28] Iqbal, Z., *et al*., Framing the Ierformance of Induced Magnetic Field and Entropy Generation on Cu and TiO_2 Nanoparticles by Using Keller Box Scheme, *Advanced Powder Technology*, *28* (2017), 9, July, pp. 2332-2345
[29] Maraj, E.N., *et al*., Viscous Dissipative Transport of a Ferrofluid (Fe_3O_4) over a Moving Surface Influenced by Magnetic Dipole and Thermal Deposition: Finite Difference Algorithm, *The European Physical Journal Plus*, *132* (2017), 11, 476
[30] Iqbal, Z., *et al*., Numerical Investigation of Nanofluidic Transport of Gyrotactic Microorganisms Submerged in Water Towards Riga Plate, *Journal of Molecular Liquids*, *234* (2017), May, pp. 296-308
[31] Azhar, E., *et al*., 2018. Numerical Approach for Stagnation Point Flow of Sutterby Fluid Impinging to Cattaneo-Christov Heat Flux Model, *Pramana*, *91* (2018), 5, 61
[32] Iqbal, Z., *et al*., The MHD Rotating Transport of CNTS in a Vertical Channel Submerged with Hall Current and Oscillations, *The European Physical Journal Plus*, *132* (2017), 3, 143
[33] Umar, M., *et al*., Numerical Treatment for the 3-D Eyring-Powell Fluid-Flow over a Stretching Sheet with Velocity Slip and Activation Energy, *Advances in Mathematical Physics*, *2019* (2019), ID 9860471
[34] Bakier, A.Y., Thermal Radiation Effect on Mixed Convection from Vertical Surfaces in Saturated Porous Media, *International Communications in Heat and Mass Transfer*, *28* (2001), 1, pp. 119-126
[35] Damseh, R. A., Magnetohydrodynamics-Mixed Convection from Radiate Vertical Isothermal Surface Embedded in a Saturated Porous Media, *Journal of Applied Mechanics*, *73* (2006), 1, pp. 54-59
[36] Hossain, M. A., Takhar, H. S., Radiation Effect on Mixed Convection Along a Vertical Plate with Uniform Surface Temperature, *Heat and Mass Transfer*, *31* (1996), 4, pp. 243-248
[37] Zahmatkesh, I., Influence of Thermal Radiation on Free Convection Inside a Porous Enclosure, *Momentum*, *10* (2007), Dec., 1
[38] Moradi, A., *et al*., On Mixed Convection-Radiation Interaction about an Inclined Plate through a Porous Medium, *International Journal of Thermal Sciences*, *64* (2013), Feb., pp. 129-136
[39] Pal, D., Mondal, H., Radiation Effects on Combined Convection over a Vertical Flat Plate Embedded in a Porous Medium of Variable Porosity, *Meccanica*, *44* (2009), 2, pp. 133-144
[40] Bahmani, A., Kargarsharifabad, H., The MHD Free Convection of Non-Newtonian Power-Law Fluids over a Uniformly Heated Horizontal Plate, *Thermal Science*, *24* (2020), 2B, pp. 1323-1334
[41] Bahmani, A., Kargarsharifabad, H., Laminar Natural-Convection of Power-Law Fluids over a Horizontal Heated Flat Plate, *Heat Transfer Asian Research*, *48* (2019), 3, pp. 1044-1066

[42] Khan, W. A., *et al*., Combined Heat and Mass Transfer of Third-Grade Nanofluids over a Convectively Heated Stretching Permeable Surface, *The Canadian Journal of Chemical Engineering*, *93* (2015), 10, pp. 1880-1888
[43] Ibrahim, W., Makinde, O. D., Magnetohydrodynamic Stagnation Point Flow of a Power-Law Nanofluid Towards a Convectively Heated Stretching Sheet with Slip, Proceedings of the Institution of Mechanical Engineers – Part E: *Journal of Process Mechanical Engineering*, *230* (2016), 5, pp. 345-354
[44] Khan, W. A., *et al*., Non-Aligned MHD Stagnation Point Flow of Variable Viscosity Nanofluids Past a Stretching Sheet with Radiative Heat, *International Journal of Heat and Mass Transfer*, *96* (2016), May, pp. 525-534
[45] Ibrahim, W., Makinde, O. D., Magnetohydrodynamic Stagnation Point Flow and Heat Transfer of Casson Nanofluid Past a Stretching Sheet with Slip and Convective Boundary Condition, *Journal of Aerospace Engineering*, 29 (2016), 2, 04015037
[46] Makinde, O. D., *et al*., Stagnation Point Flow of MHD Chemically Reacting Nanofluid over a Stretching Convective Surface with Slip and Radiative Heat, Proceedings of the Institution of Mechanical Engineers, Part E: *Journal of Process Mechanical Engineering*, *231* (2017), 4, pp. 695-703
[47] Makinde, O. D., *et al*., Buoyancy Effects on MHD Stagnation Point Flow and Heat Transfer of a Nanofluid Past a Convectively Heated Stretching/Shrinking Sheet, *International Journal of Heat and Mass Transfer*, *62* (2013), July, pp. 526-533
[48] Azhar, E., *et al*., Numerical Approach for Stagnation Point Flow of Sutterby Fluid Impinging to Cattaneo-Christov Heat Flux Model, *Pramana*, *91* (2018), 5, 61

Paper submitted: December 7, 2019
Paper revised: May 2, 2020
Paper accepted: May 5, 2020